Arrhythmogenic Ca^{2+} Signaling in a Metabolic Model of HFpEF

Aaron D. Kaplan[1,2], Liron Boyman[1,3,4], Christopher W. Ward[1,5,6], W. Jonathan Lederer[1,3,4], Maura Greiser[1,3,6]*

[1] Center for Biomedical Engineering and Technology, University of Maryland School of Medicine, Baltimore, Maryland, USA.

[2] Division of Cardiovascular Medicine, Department of Medicine, University of Maryland School of Medicine, Baltimore, Maryland, USA

[3] Department of Physiology, University of Maryland School of Medicine, Baltimore, Maryland, USA.

[4] Greenebaum Comprehensive Cancer Center, University of Maryland School of Medicine, Baltimore, Maryland, USA

[5] Department of Orthopedics, University of Maryland School of Medicine, Baltimore, Maryland, USA.

[6] Claude D. Pepper Older Americans Independence Center, University of Maryland School of Medicine, Baltimore, Maryland, USA.

* Corresponding author

Short Title: Ca^{2+}-based Arrhythmias in HFpEF

Correspondence to:

Maura Greiser, MD, PhD
Center for Biomedical Engineering and Technology & Department of Physiology
University of Maryland School of Medicine
111 S. Penn Street
Baltimore, MD 21201
USA
Phone: +410-706-1567
Fax: + 410-706-8184
email: mGreiser@som.umaryland.edu

Abstract

Heart failure with preserved ejection fraction (HFpEF) already represents approximately 50% of all cases of heart failure and its incidence continues to rise. Initially regarded as a disorder of hypertensive left ventricular dysfunction in older adults, HFpEF has emerged as a complex cardiometabolic syndrome in younger adults associated with other co-morbidities such as obesity, decreased insulin sensitivity, dyslipidemia and others. An important part of the high morbidity and mortality associated with HFpEF is a high rate of sudden cardiac death (~ 25%) and malignant arrhythmias whose underlying mechanisms remain poorly understood. Here we have developed a three 'hit' model of metabolic-stress induced HFpEF in C57BL6/J mice (HFpEF mice) by adding high dietary fructose to the well-established two 'hit' HFpEF model that is based on a high fat diet plus nitric oxide synthase inhibition with L-NAME. Importantly, after 5 months, all HFpEF animals developed premature ventricular contractions (PVCs) and 50% showed episodes of sustained ventricular tachycardia (VT) after low-dose systemic isoproterenol treatment, while none of the control animals developed either PVCs or VT. We report that in isolated cardiac myocytes from HFpEF mice the incidence of spontaneous Ca^{2+} release events or Ca^{2+} sparks, is increased 9-fold compared to age-matched controls. This massive increase in spontaneous Ca^{2+} release from the sarcoplasmic reticulum is reflected in a 7-fold increase in spontaneous Ca^{2+} waves in cardiac myocytes from HFpEF mice when compared to controls. Surprisingly, in contrast to the changes documented in intracellular Ca^{2+} homeostasis in heart failure with reduced ejection fraction (HFrEF), the diastolic intracellular Ca^{2+} concentration ($[Ca^{2+}]_i$) in cells from HFpEF mice was not increased and stimulated Ca^{2+} transients (CaT) had a higher amplitude than control myocytes. Taken together, here we demonstrate for the first time that arrhythmogenic intracellular Ca^{2+} signaling likely underlies the malignant ventricular arrhythmias seen in metabolic HFpEF. Our findings also provide direct evidence that the cellular and molecular mechanisms of Ca^{2+} based arrhythmogenesis in HFpEF are distinct from the processes known to occur in HFrEF.

Research Letter

Heart failure (HF) with preserved ejection fraction (HFpEF) is a widely prevalent form of HF which confers significant morbidity and mortality[1]. Initially considered a disorder of diastolic dysfunction in older adults related to hypertensive left-ventricular remodeling, the incidence of HFpEF is now rapidly growing in younger adults driven by metabolic and inflammatory stress from overlapping comorbidities of obesity, dyslipidemia, hypertension and decreased insulin sensitivity (i.e., pre-diabetes)[1]. Ventricular tachycardia (VT) and a high rate of sudden cardiac death (~25%) are major contributors to HFpEF morbidity and mortality[1]. Anti-arrhythmic treatment options in HFpEF remain limited because the underlying arrhythmia mechanisms are poorly understood. To address this critical gap in our understanding, we produced a metabolic stress-induced HFpEF model in mice that is highly arrhythmogenic. Metabolic and hypertensive stress was induced in C57BL6/J mice by adding high dietary fructose (20% of dietary Kcals) to the well-established "two-hit" murine HFpEF model[2] (high-fat diet plus nitric oxide synthase inhibition with L-NAME). 5 months of this "three-hit" intervention effectively increased adiposity (Fig. A) and decreased insulin sensitivity without overt type 2 diabetes (Fig. B). Together with left ventricular hypertrophy, preserved ejection fraction, elevated cardiac strain (Fig. C) and increased serum levels of brain natriuretic peptide (BNP, Fig. D) this model effectively replicates key aspects of the clinical HFpEF phenotype. Importantly, application of low-dose isoproterenol (5mg/kg body weight) induced arrhythmogenic PVCs in all HFpEF animals and triggered sustained VT in 50% of HFpEF animals while age-matched control animals did not develop either (Fig. E).

Although a distinct pattern of arrhythmogenic intracellular Ca^{2+} signaling is central to the malignant VTs in heart failure with reduced ejection fraction (HFrEF)[3], arrhythmogenic Ca^{2+} signaling has not been assessed in metabolic stress-induced models of HFpEF. Here, we show that in isolated ventricular myocytes from HFpEF mice (HFpEF myocytes) the frequency of Ca^{2+} sparks was massively (~ 10fold) increased. Similarly, the Ca^{2+} spark mediated leak of Ca^{2+} from the sarcoplasmic reticulum (SR) was increased 9fold. The Ca^{2+} spark amplitude in HFpEF myocytes was also higher than in control myocytes isolated from age-matched control mice (CTL myocytes, Fig. F). Consistent with the massive increase in Ca^{2+} sparks and Ca^{2+} spark mediated SR Ca^{2+} leak, the frequency of spontaneous, arrhythmogenic Ca^{2+} waves was 7fold higher in HFpEF myocytes compared to CTL myocytes (Fig. G.iii). In addition, the Ca^{2+} wave-free survival was much shorter in HFpEF myocytes providing further evidence for the high burden of arrhythmogenic Ca^{2+} release from the SR in HFpEF (Fig. G.iv). To test whether the increased *in-vivo* sensitivity to β-adrenergic arrhythmias in HFpEF mice (Fig. E) was driven by increased β-adrenergic sensitivity of the myocyte, we applied low dose isoproterenol (50 nmol/L) to myocytes *in vitro*. Here we show isoproterenol's impact on arrhythmogenic Ca^{2+} wave frequency was 2-fold greater in HFpEF versus CTL myocytes (Fig. G.v).

In search for underlying mechanisms, we examined the ultrastructure of the transverse and axial tubular system (TATS) of living cardiomyocytes. Sub-diffraction Airy scan imaging revealed no changes in TATS density, organization or orientation (Fig. H) in HFpEF which is contrary to HFrEF where reduced TATs density is a well-established contributor to arrhythmogenic Ca^{2+} signaling[4]. The stimulated Ca^{2+} transient (CaT) amplitude was increased in HFpEF myocytes (Fig. F) and CaT decay was faster

in HFpEF myocytes at 1 Hz but unchanged at the more physiological rate of 4 Hz (Fig. H). A crucial underlying mechanism of Ca^{2+} based arrhythmogenesis in HFrEF is a higher diastolic Ca^{2+} concentration in the cytosol ($[Ca^{2+}]_i$), which increases the sensitivity of the SR's Ca^{2+} release channels, the ryanodine receptors type 2, to release Ca^{2+} [3]. We used the ratiometric Ca^{2+} indicator Fura-2 and calibrated each individual cell to measure $[Ca^{2+}]_i$ (Fig. J). Surprisingly, diastolic $[Ca^{2+}]_i$ was not increased in HFpEF myocytes at physiological stimulation rates and even was lower than in CTL myocytes at 0.5 Hz (J.ii), while systolic $[Ca^{2+}]_i$ was higher in HFpEF myocytes (Fig. J.iii). Finally, Western Blot analyses of Ca^{2+} handling proteins revealed a reduction in the expression and phosphorylation of phospholamban (PLB), the regulatory protein of the SR Ca^{2+} ATPase (Fig. K). In addition, the protein expression levels of calsequestrin2 (CSQ2), the major intra SR Ca^{2+} buffering protein were reduced (Fig. K). Even small reductions of CSQ2 and thus the SR's capacity to bind Ca^{2+} can produce significant Ca^{2+} dependent arrhythmia burden [5].

Here we report arrhythmogenic intracellular Ca^{2+} signaling in a model of metabolic stress-induced HFpEF with high arrhythmia burden. These findings suggest that arrhythmogenic intracellular Ca^{2+} signaling likely contributes to malignant arrhythmias in patients with HFpEF. We report changes in Ca^{2+} signaling that are distinct from the changes known to occur in HFrEF. Specifically, we show that the arrhythmogenic Ca^{2+} waves in HFpEF are not triggered by increased diastolic $[Ca^{2+}]_i$, nor by loss of TATS density, but might be related to reduced intra SR Ca^{2+} buffering capacity. These findings stress the need for further elucidation of the mechanisms underlying this novel Ca^{2+} based arrhythmogenesis as a crucial step for the identification of novel treatment targets for HFpEF-associated arrhythmias.

Sources of Funding: 7U19 AI090959 (WJL &LB); Frontiers in Anesthesia Research Award from International Anesthesia Research Society (WJL & LB); R01 HL142290 (WJL &CWW); 5R35GM140822 (WJL); U01 HL116321 (WJL); Special BioMET/UMB Funds (WJL). University of Maryland Claude D. Pepper Center Grant P30 AG028747 (MG). R01 AR071618 (CWW).

Disclosures: None.

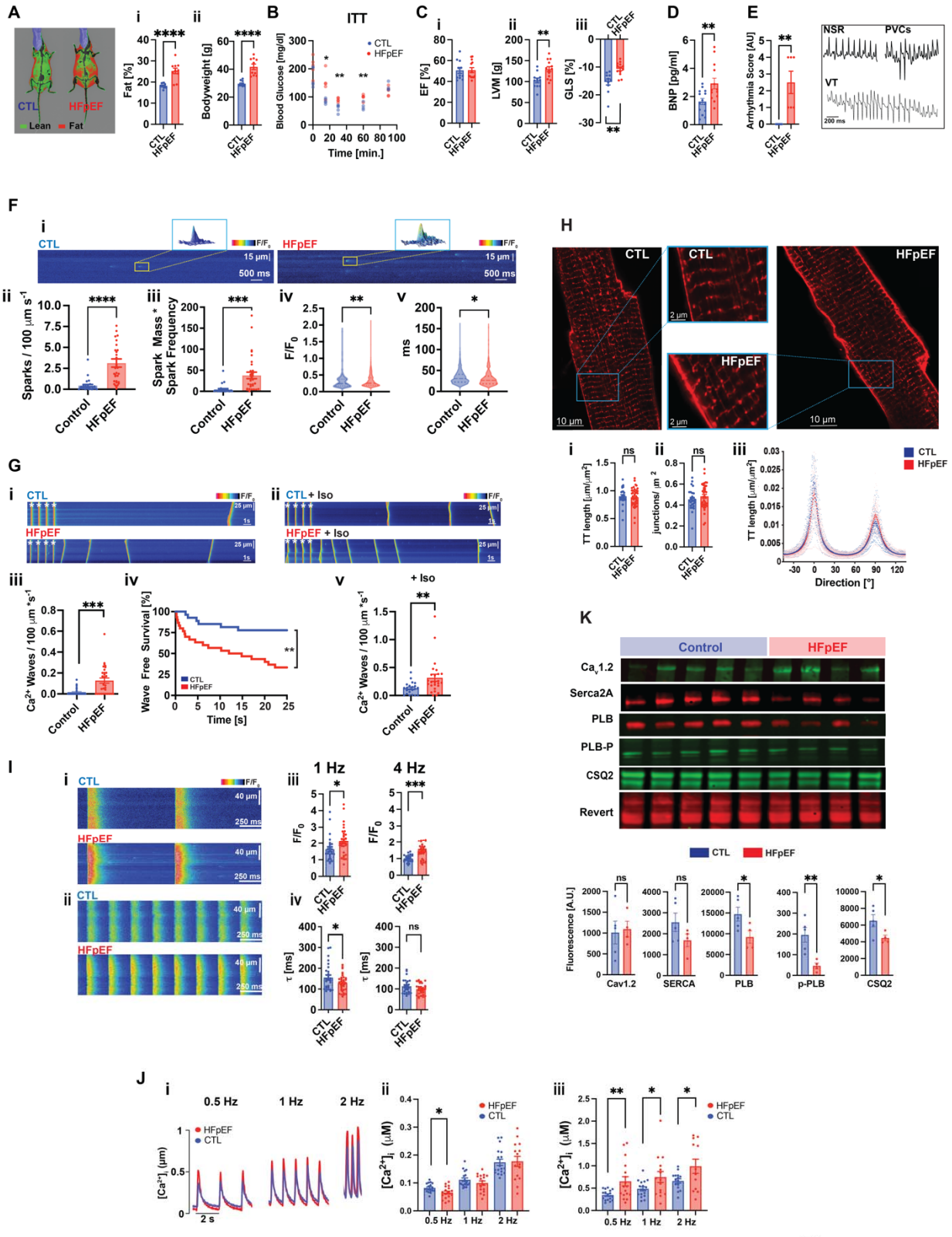
A
CTL
HFpEF
Lean
Fat
Fat [%]
Bodyweight [g]
B
ITT
Blood Glucose [mg/dl]
Time [min.]
C
EF [%]
LVM [g]
GLS [%]
D
BNP [pg/ml]
E
Arrhythmia Score [AU]
NSR
PVCs
VT
F
Sparks / 100 µm s-1
Spark Mass * Spark Frequency
F/F0
ms
Control
G
CTL + Iso
HFpEF + Iso
Ca2+ Waves / 100 µm *s-1
Wave Free Survival [%]
Time [s]
H
TT length [µm/µm2]
junctions/ µm 2
Direction [°]
I
1 Hz
4 Hz
τ [ms]
J
0.5 Hz
1 Hz
2 Hz
[Ca2+]i (µM)
K
Control
HFpEF
Cav1.2
Serca2A
PLB
PLB-P
CSQ2
Revert
Fluorescence [A.U.]
SERCA
p-PLB

Figure

References

1. Borlaug BA, Sharma K, Shah SJ and Ho JE. Heart Failure With Preserved Ejection Fraction: JACC Scientific Statement. *Journal of the American College of Cardiology*. 2023;81:1810-1834.
2. Schiattarella GG, Altamirano F, Tong D, French KM, Villalobos E, Kim SY, Luo X, Jiang N, May HI, Wang ZV, Hill TM, Mammen PPA, Huang J, Lee DI, Hahn VS, Sharma K, Kass DA, Lavandero S, Gillette TG and Hill JA. Nitrosative stress drives heart failure with preserved ejection fraction. *Nature*. 2019;568:351-356.
3. Gomez AM, Valdivia HH, Cheng H, Lederer MR, Santana LF, Cannell MB, McCune SA, Altschuld RA and Lederer WJ. Defective excitation-contraction coupling in experimental cardiac hypertrophy and heart failure. *Science*. 1997;276:800-6.
4. Zhang C, Chen B, Guo A, Zhu Y, Miller JD, Gao S, Yuan C, Kutschke W, Zimmerman K, Weiss RM, Wehrens XH, Hong J, Johnson FL, Santana LF, Anderson ME and Song LS. Microtubule-mediated defects in junctophilin-2 trafficking contribute to myocyte transverse-tubule remodeling and Ca2+ handling dysfunction in heart failure. *Circulation*. 2014;129:1742-50.
5. Chopra N, Kannankeril PJ, Yang T, Hlaing T, Holinstat I, Ettensohn K, Pfeifer K, Akin B, Jones LR, Franzini-Armstrong C and Knollmann BC. Modest reductions of cardiac calsequestrin increase sarcoplasmic reticulum Ca2+ leak independent of luminal Ca2+ and trigger ventricular arrhythmias in mice. *Circ Res*. 2007;101:617-26.

Figure Legend

Figure. Arrhythmogenic Ca^{2+} signaling in metabolic HFpEF.
All experiments involving animals were approved by the Institutional Animal Care and Use Committee of the University of Maryland School of Medicine, Baltimore, Maryland. Statistical analysis was performed using GraphPad Prism v9 and Matlab. Results are presented as mean±SEM. No statistical analyses were performed to predetermine sample sizes; estimates were made on the basis of our previous experience, experimental approach, and availability and feasibility required to obtain statistically significant results. When representative images are shown, the selected images are those that most accurately represent the average data obtained in all samples. **A**. Body composition was quantified *in vivo* with an iNSIGHT DXA (Scintica, Canada) using dual x-ray absorptiometry. **i.** Fat and **ii**. Bodyweight. **B**. Insulin tolerance test (ITT) was performed (0.5 U/kg recombinant human insulin I.P) after a 4 hour fast with glucose monitored (Contour Next One; time 0, 15, 30, 60 90min) from tail blood in HFpEF (n=5) and control (n=5) mice. **C**. Transthoracic echocardiography was performed using a Vevo 2100 (VisualSonics, Canada). **i**. Ejection fraction (EF), **ii.** Left ventricular mass (LVM) and **iii.** Global longitudinal strain (GLS) were measured in HFpEF (n=13) and control (n=11) animals. **: $p<0.01$. **D.** Serum levels of B-type natriuretic peptide (BNP) in HFpEF (n=8) and control mice (n=7). BNP was measured quantitatively (pg/mL) using an ELISA assay (RayBiotech, USA). **E.** EKGs were recorded in awake HFpEF (n=6) and control (n=6) mice using an EMKA tunnel system (Emka Technologies). Mice were injected (i.p.) with isoproterenol (5mg/kg body weight) and EKGs were recorded for 1 h. An arrhythmia score was assigned to each animal (0 : no arrhythmias, 1: single PVCs, 2: coupled PVCs, 3: triple PVCs or non-sustained VT, 4: sustained VT). **: $p<0.01$. Unpaired *t* test. Original ECG recordings show examples for normal sinus rhythm (NSR), premature ventricular contractions PVCs) and ventricular tachycardia (VT). **F.** Ca^{2+} sparks in HFpEF. Ca^{2+} sparks were recorded in freshly isolated ventricular myocytes from HFpEF (n=4) and control (n=4) mice using the Ca^{2+} indicator fluo4-AM (1-5 µmol/L) on an inverted Nikon A1R confocal laser scanning microscope. Spontaneous Ca^{2+} sparks were recorded after steady-state external field stimulation at 1 Hz. **i.** Left panel: Exemplar of Ca^{2+} sparks in a line scan recording from a control myocyte (CTL). Right panel: Exemplar of Ca^{2+} sparks in a line scan recording from a HFpEF myocyte. **ii.** Ca^{2+} spark frequency, **iii.** Ca^{2+} spark-mediated SR Ca^{2+}leak, **iv.** Ca^{2+} spark amplitude, **v.** Ca^{2+} spark duration as full duration half maximum (FDHM). ****: $p<0.0001$; ***: $p<0.001$; **: $p<0.01$; *: $p<0.05$. **G.** Ca^{2+} waves in HFpEF at baseline and after treatment with isoproterenol (50 nmol/L). Ca^{2+} waves were recorded in freshly isolated ventricular myocytes from HFpEF (n=4) and control (n=4) mice before and after treatment with 50 nmol/L isoproterenol using the Ca^{2+} indicator fluo4-AM (1-5 µmol/L) on an inverted Nikon A1R confocal laser scanning microscope. Cells underwent external-field stimulation at 1 Hz to ensure comparable SR Ca^{2+} loading. **i.** Top panel: Exemplar of spontaneous Ca^{2+} waves in a confocal line scan from a control myocyte. Bottom: exemplar of spontaneous Ca^{2+} waves in a confocal line scan from a control myocyte after isoproterenol treatment. * denotes stimulated beat. **ii**. Top panel: Exemplar of spontaneous Ca^{2+} waves in a confocal line scan from a HFpEF myocyte. Bottom panel: Exemplar of spontaneous Ca^{2+} waves in a confocal line scan from a

HFpEF myocyte after isoproterenol treatment. * denotes stimulated beat. **iii.** Spontaneous Ca^{2+} wave frequency in untreated HFpEF and control myocytes, **iv.** Ca^{2+} wave free survival in HFpEF and control myocytes, **v.** Spontaneous Ca^{2+} wave frequency in HFpEF and control myocytes after treatment with isoproterenol. ***: $p<0.001$; **: $p<0.01$. **H.** Transverse-Axial Tubule system (TATS) in HFpEF myocytes. **i.** Deconvolved sub-diffraction AiryScan images of living ventricular myocytes stained with the membrane dye di-8-ANEPPS (5 µmol/L) to label the TATS. Left image shows the TATS in a myocyte from control mice (n=3), right image shows TATS in a myocyte from mice with HFpEF (n=4). Middle panels show the magnified view of the sub-cellular regions within the blue outlines. **ii.** Total length of the TATS within cells. **iii.** Number of junctions that connect intersecting perpendicular tubules. **iv.** The length of the TATS at each direction within the cells. Tubules oriented at about 0 degrees are tracking the long axis (longitudinal) of ventricular myocytes, tubules oriented at about 90 are transverse. The analysis was conducted within the interior space of the cell, excluding the surface membrane and nuclei. It included binarization of deconvolved AiryScan images, image skeletonization, and quantification of length, orientation, and connecting junctions per mm^2 of intracellular space via the skeleton analysis plugin of the Fiji software (NIH). **I.** Ca^{2+} transients (CaT) in HFpEF myocytes. CaT were recorded in freshly isolated ventricular myocytes from HFpEF (n=4) and control (n=4) mice using the Ca^{2+} indicator fluo4-AM (1-5 µmol/L). CaTs were elicited by external field stimulation and recorded on an inverted Nikon A1R confocal laser scanning microscope. **i.** Exemplars of stimulated CaTs at 1 Hz. Top panel: Original line scan of stimulated CaTs from a control myocyte. Bottom panel: Original line scan of stimulated CaTs from a HFpEF myocyte. **ii.** Exemplars of stimulated CaTs at 4 Hz. Top panel: Original line scan of stimulated CaTs from a control myocyte. Bottom panel: Original line scan of stimulated CaTs from a HFpEF myocyte. **iii.** CaT amplitude (F/F_0) in HFpEF and control myocytes at 1 Hz (left panel) and 4 Hz (right panel). **iv.** CaT decay (ms) in HFpEF and control myocytes at 1 Hz (left panel) and 4 Hz (right panel). **J.** $[Ca^{2+}]_i$ in HFpEF myocytes. CaTs were elicited by external field stimualtion and measured using the ratiometric Ca^{2+} indicator fura2-AM (7 µmol/L). Wide field imaging was achieved with a 40X objective (Nikon S Fluor, Oil, 1.30 NA) using two excitation wavelengths (340 nm and 380 nm) by fast switching scanning mirrors and narrow bandwidth excitation filters (340 nm ± 10 nm; 380 nm ± 10 nm, DG 5, Sutter Instrument). Emission light was collected at 510 ± 40 nm. Data were acquired using Nikon NIS- Elements software. $[Ca^{2+}]_i$ was calibrated in the recording of each cell after the end of the experiment. **i.** Original recordings of CaTs in myocytes from control and HFpEF mice (0.5-2 Hz). **ii.** Diastolic $[Ca^{2+}]_i$ in myocytes from control and HFpEF mice (0.5-2 Hz). **iii.** Systolic $[Ca^{2+}]_i$ in myocytes from control and HFpEF mice. **K.** Protein expression levels of key Ca^{2+} handling proteins in HFpEF. Clarified protein homogenates from left ventricle (5 mg total protein) were size separated by SDS Page and probed by Western blot using NIR fluorescent secondary antibodies and Licor Revert total protein detection. Membranes were imaged on a Licor Clx imager (Li-Cor Biosciences, USA) with antibody fluorescence quantification, normalized to total protein, using Licor ImageStudio. $Ca_V1.2$: α1c subunit of the L-type Ca^{2+} channel, SERCA: SR Ca^{2+} ATPase, PLB: phospholamban, PLB-P: phosphorylated-PLM, CSQ2: calsequestrin 2).